Published in final edited form as:
Alcohol Clin Exp Res. 2013 October ; 37(10): 1668–1679. doi:10.1111/acer.12157.

Genetic resistance to liver fibrosis on A/J mouse chromosome 17

David A. DeSantis[1], **Peter Lee**[1], **Stephanie K. Doerner**[2], **Chih-wei Ko**[1], **Jean H. Kawasoe**[2], **Annie E. Hill-Baskin**[2], **Sheila R. Ernest**[2], **Prerna Bhargava**[6], **Kyu Yeon Hur**[6], **Gail A. Cresci**[3], **Michele T. Pritchard**[5], **Chih-Hao Lee**[6], **Laura E. Nagy**[1,3,*], **Joseph H. Nadeau**[4], and **Colleen M. Croniger**[1,*]

[1]Department of Nutrition, Case Western Reserve University School of Medicine, Cleveland, Ohio 44106

[2]Department of Genetics, Case Western Reserve University School of Medicine, Cleveland, Ohio 44106

[3]Departments of Pathobiology and Gastroenterology, Cleveland Clinic Foundation, Cleveland Ohio 44106

[4]Institute for Systems Biology, Seattle, WA 98109

[5]Departments of Pharmacology, Toxicology and Therapeutics, The University of Kansas Medical Center, Kansas City, KS 66160

[6]Deptartment of Genetics and Complex Diseases, Harvard University School of Public Health, Boston, MA 02115

Abstract

Background—Because the histological and biochemical progression of liver disease is similar in alcoholic steatohepatitis (ASH) and nonalcoholic steatohepatitis (NASH), we hypothesized that the genetic susceptibility to these liver diseases would be similar. To identify potential candidate genes that regulate the development of liver fibrosis, we studied a chromosome substitution strain (CSS-17) that contains chromosome 17 from the A/J inbred strain substituted for the corresponding chromosome on the C57BL/6J (B6) genetic background. Previously we identified quantitative trait loci (QTLs) in CSS-17, namely obesity resistant QTL13 and QTL 15 (*Obrq13 and Obrq15,* respectively), that were associated with protection from diet-induced obesity and hepatic steatosis on a high fat diet.

Methods—To test if these or other CSS-17 QTLs conferred resistance to alcohol-induced liver injury and fibrosis, B6, A/J, CSS-17 and congenics 17C-1 and 17C-6 were either fed Lieber DeCarli ethanol-containing diet or had carbon tetrachloride (CCl_4) administered chronically.

Results—The congenic strain carrying *Obrq15* showed resistance from alcohol-induced liver injury and liver fibrosis, whereas *Obrq13* conferred susceptibility to liver fibrosis. From published deep sequencing data for chromosome 17 in the B6 and A/J strains, we identified candidate genes in *Obrq 13* and *Obrq15* that contained single nucleotide polymorphisms (SNPs) in the promoter region or within the gene itself. NADPH oxidase organizer 1 (*Noxo1*) and NLR family, CARD

*Work supported by: National Institue on Alcohol Abuse and Alcoholism (NIAAA) P-20 Grant-AA017837 (LEN and CMC), AA017918 (MTP), 1F32AA021044-02 (GAC) and a grant from Howard Hughes Medical Institute for Undergraduate Research (PL).

Corresponding Author: Colleen M. Croniger, Ph.D., Case Western Reserve University - Nutrition, 10900 Euclid Ave, Cleveland, Ohio 44106, United States, cmc6@case.edu.

domain containing 4 (*Nlrc4*) showed altered hepatic gene expression in strains with the A/J allele at the end of the ethanol diet study and after CCl_4 treatment.

Conclusion—Aspects of the genetics for the progression of ASH are unique compared to NASH, suggesting that the molecular mechanisms for the progression of disease are at least partially distinct. Using these CSSs we identified two candidate genes, *Noxo1* and *Nlrc4,* which modulate genetic susceptibility in ASH.

Keywords

C57BL/6J; A/J; congenic strains; liver fibrosis; Nlrc4 inflammasome; CCl_4

Introduction

The main causes of liver disease in industrialized countries include alcoholic steatohepatitis (ASH), chronic hepatitis C virus (HCV) infection, and nonalcoholic steatohepatitis (NASH) (Gines et al., 2004). In patients who chronically consume alcohol or are morbidly obese, the progression of liver disease is similar, originating with development of a fatty liver (hepatic steatosis) and then progresses to hepatitis, fibrosis and finally cirrhosis. However, of those patients that develop hepatitis, only a small subset will progress further to cirrhosis. Approximately 20–50% of patients with ASH and ~20% of patients with NASH will progress to cirrhosis (Diehl et al., 1988) suggesting a gene-environment interaction contributes to disease progression.

Although most genetic screens focus on the behavioral aspect of alcohol dependence, several investigated the genetic susceptibility to liver injury (Kimura and Higuchi, 2011; Lin et al., 2012). Recently, both genetic and environmental risk factors are known to influence not only addictive behavior but also the severity of steatosis, hepatitis, and liver fibrosis. In human studies, SNPs have been identified in genes known for the metabolism of alcohol, l such as alcohol dehydrogenase (ADH) (Edenberg et al., 2006; Xuei et al., 2006), aldehyde dehydrogenase (ALDH) (Vasiliou et al., 2000), and cytochrome P450, family 2, subfamily E, polypeptide 1 (CYP2E1) (Itoga et al., 2001; Webb et al., 2011). This list of candidate genes for liver fibrosis is not comprehensive, but it supports the concept that polymorphisms in multiple genes impact the progression of liver injury and disease. In addition there are other mechanisms besides genetic modifications (such as SNPs) that could modulate development of disease. For example, epigenetic regulation and microRNAs could also be genetically regulated and impact disease progression.

Using an unbiased approach to find genes that modulate the development of fibrosis, we surveyed chromosomal substitution strains (CSSs) containing chromosome 17 from the A/J inbred strain that was substituted for the corresponding chromosome on the C57BL/6J (B6) genetic background. CCS-17 was chosen because this strain is resistant to obesity and steatosis on a high fat, simple-carbohydrate diet (HFSC) and we previously located several quantitative trait loci (QTLs) associated with obesity and hepatic steatosis (Millward et al., 2009). Two of the identified QTLs associated with resistance to diet-induced obesity and hepatic steatosis on HFSC diet are *Obrq13* and *Obrq15* (Figure 1, Table 2) (Millward et al., 2009). The primary difference between these QTLs derived from A/J alleles is that *Obrq15,* develops insulin resistance on the HFSC diet, whereas *Obrq13* remains insulin sensitive as measured by glucose tolerance tests and calculated homeostasis model of insulin resistance (HOMA-IR). Since progression of liver disease is similar in NASH and ASH, we hypothesized that the genetic susceptibility to these liver diseases would be the similar. We hypothesized that *Obrq13* and *Obrq15* would also confer resistance to alcohol-induced liver injury and fibrosis. In this study, congenic strains derived from CSS-17 that contain Obrq13

(called 17C-1) or *Obrq15* (called 17C-6) were analyzed for their susceptibility to either alcohol-induced liver injury or carbon tetrachloride (CCl_4) induced liver fibrosis.

Experimental Procedures

Husbandry

C57BL/6J (B6), A/J, and B6-Chr $17^{A/J}$/NaJ (CSS-17) mice were generated and maintained at Case Western Reserve University (Singer et al., 2004). The congenic strains derived from CSS-17 were generated as previously described (Millward et al., 2009). Mice were raised in microisolator cages with a 12 hour light: 12 hour dark cycle. All mice were weaned at 3–4 weeks of age and raised on LabDiet #5010 autoclavable rodent chow (LabDiet, Richmond, IN) *ad libitum* until studies were initiated.

Ethanol Feeding Diet Study

Eight to ten week-old female B6, A/J, CSS-17 and congenics 17C-1 and 17C-6 were fed either Lieber DeCarli ethanol-containing diet (+EtOH) or pair fed control diet (PF) as previously described (16). For measurements of serum ethanol concentrations, blood was taken from the tail-vein 2hr into the feeding cycle. Female mice were used for this study because they are more susceptible to alcohol-induced liver injury and have a significantly higher risk of developing cirrhosis for any given level of alcohol intake (Sato et al., 2001).

CCl_4 administration and sample collection

CCl_4 (Sigma-Aldrich; St. Louis, MO) administration in male B6, A/J, CSS-17 and congenics 17C-1 and 17C-6 strains was performed as previously described (Pritchard and Nagy, 2010). We used male mice for this study because our previous study to identify QTLs for resistance to diet-induced obesity was performed in male mice (Millward et al., 2009) due to their greater propensity of gaining body weight than females on HFSC diet (Hong et al., 2009). Therefore, to compare our previous high fat diet study to development of liver fibrosis, the CCl_4 was administered to male mice.

Histology and Immunohistochemistry

For histological analysis, formalin-fixed tissues were paraffin-embedded, sectioned (5μm) and stained with Sirius red stain for collagen as previously described (Pritchard and Nagy, 2010). Formalin-fixed, paraffin-embedded liver sections were de-paraffinized and stained for α smooth muscle actin (α-SMA) as previously described (Pritchard and Nagy, 2010). The positive α-SMA areas and Sirius Red Stained areas were morphometrically quantified using Image-Pro Plus software (Media Cybernetics, Bethesda, MD) and analyzed. All images presented in the results are representative of at least 3 images per liver and 4 mice per experimental condition.

Neutrophils were immunolocalized in liver tissue using an anti-neutrophil antibody, NIMP-R14 (Abcam, Cambridge, MA). Briefly, formalin-fixed, paraffin-embedded liver tissues were de-paraffinized. Liver sections were then incubated with the NIMP-R14 antibody (1:100) overnight at 4°C. After washing, the tissues were incubated with a biotinylated anti-rat secondary antibody according to the manufacturer's instructions (Vectastain Elite ABC kit, rat IgG, Vector Laboratories, Burlingame, CA). Subsequently, tissues were incubated with an Avidin-biotin-HRP complex (Vectastain Elite ABC kit). ImmPACT NovaRed peroxidase substrate was utilized to visualize positive staining in tissues. To quantify neutrophils content in tissues, 10 non-overlapping images of each section were captured and neutrophils presence was graded as none, rare, few or moderate. These subjective assessments were assigned a number (none = 0, rare = 2, few = 4, moderate = 6) and each

section's numbers were averaged. The averages (a single number per mouse) were used for statistical analysis.

Measurement of hepatic triglycerides, plasma ethanol, plasma alanine aminotransferase (ALT) concentrations

For measurement of liver triglycerides, 100–200 mg of liver was saponified with an equal volume by weight of 3M KOH/65% ethanol as described (Salmon and Flatt, 1985). We measured glycerol concentration against glycerol standards, using a commercially available triglyceride glycerol phosphate oxidase (GPO) reagent kit (Pointe Scientific, Lincoln Park, MI), as previously described (Buchner et al., 2008). Plasma ethanol concentration and ALT were measured using commercially available enzymatic assay kits (Sigma-Aldrich, St. Louis, MO), according to manufacturer's instructions.

Isolation of Hepatocytes

Hepatocytes were isolated from C57/Bl6, 17C-1 and 17C-6 mice by an *in situ* collagenase (type VI; Sigma, St. Louis, Mo.) perfusion technique, as described previously (West et al., 1989). Hepatocytes were separated from the nonparenchymal cells by two cycles of differential centrifugation (50 × g for 2 min) and further purified over a 30% Percoll gradient. The purity of these hepatocyte cultures exceeded 98% by light microscopy, and viability was typically more than 95% by trypan blue exclusion assay. The cells were isolated and mRNA was harvested without culturing.

Isolation of Hepatic Stellate Cells

Mouse hepatic stellate cells (HSC) were isolated from B6, 17C-1 and 17C-6 mice by enzymatic digestion and Percoll density gradient centrifugation, as previously described (Blomhoff and Berg, 1990). HSC were isolated and mRNA was harvested without culturing the cells for the day zero (quiescent HSC). HSCs were cultured for seven days (activated HSCs) in 6 well plates with Dulbecco's modified Eagle medium (DMEM) containing 10% fetal bovine serum (FBS), glutamine, HEPES buffer, and antibiotics. The cells were incubated at 37°C in an air atmosphere containing 5% CO_2. After 7 days the cells were isolated and we extracted mRNA for day 7 values (Blomhoff and Berg, 1990).

Isolation of Macrophages

Peritoneal macrophages were obtained by peritoneal lavage from C57/Bl6, 17C-1 and 17C-6 mice that were injected with 2 ml of 4% thioglycollate. Thioglycollate-elicited peritoneal macrophages (IPDM) were collected from the peritoneal cavity of mice three days after injection. Macrophages were collected by centrifugation and plated (Corning, Lowell, MA) in RPMI- 1640 medium (Sigma-Aldrich, St. Louis, MO) supplemented in 10% fetal calf serum (FCS), 300 mg/L L-glutamine (Sigma), 100 U/ml penicillin/0.1 mg/ml streptomycin (Sigma), and 1 mM sodium pyruvate (Sigma). The cells were incubated at 37°C in an air atmosphere containing 5% CO2. Unattached cells were removed by refreshing the medium 4 hr after isolation. After culture for 20 hr, cell culture media was removed and replaced with fresh media and were stimulated with 100 ng/ml lipopolysaccharide (LPS). After 4 hr stimulation with LPS, cell culture media were removed and cells were collected for isolation of RNA.

Isolation of Bone Marrow Derived Macrophages and Measurement of ROS

Bone marrow derived macrophages (BMDMs) were differentiated from femoral bone marrow cells with 20% of L929 conditioned medium in DMEM medium (Sigma, St. Louis, MO). Every other day, the medium was replaced with the fresh medium. On day 7–8, cells were collected with enzyme free cell dissociation buffer (Gibco Life Technologies, Grand

Island, NY). To measure cellular reactive oxygen species (ROS) the cells were incubated with 10um of Cm-H2DCFDA (#C6827, Invitrogen, Grand Island, NY), in HBSS for 1hr. Fluorescence was measured by fluorescence activated cell sorting (FACS) analysis. Values were expressed as Mean Fluorescent Intensity (MFI) X %Gated.

Real-time quantitative reverse transcription PCR (Real-Time qRT-PCR)

Total RNA from 30 mg of liver or isolated cells was prepared with an RNeasy Mini kit (Qiagen, Valencia, CA) and was synthesized to single-strand cDNA from 500 ng of total RNA with random hexamer primers and MMTV reverse transcriptase (Applied Biosystems, Foster City, CA). We amplified cDNAs using SYBR Green PCR Core reagent mix (Applied Biosystems, Foster City, CA), performed real-time qRT-PCR with a Chromo4 Cycler (MJ Research). The relative amounts of mRNA were determined by the ΔCt values [mean Ct gene of interest mean Ct from 18S rRNA or 36b4 (housekeeping gene) from the same mouse] as previously described (Millward et al., 2009; Pritchard et al., 2011).

Protein isolation and Western Blotting

Proteins were isolated and Western Blot analysis was performed from liver samples as previously described (Millward et al., 2010). The membranes were incubated with antibodies to CYP2E-1 (1:10,000; Fitzgerald Industries International Concord, MA) or αSMA (1:5,000;Santa Cruz Biotechnology, Santa Cruz, CA) The immunoreactive proteins were detected using the Super-Signal Chemiluminescent Substrate® Kit, and measured the density of the immunoreactive bands by scanning densitometry (UN-SCAN-IT gel software, Orem, Utah). The membranes were stripped and normalized for loading differences using heat shock cognate-70 (HSC70) (1:16,000; Santa Cruz Biotechnology, Santa Cruz, CA) as previously described (Millward et al., 2010).

Statistical Analysis

The values reported are means± standard error of the mean (SEM). Data were analyzed with Student-*t* test or ANOVA with Bonferonni's correction for multiple testing using GraphPad Prism (GraphPad Software, San Diego CA).

Results

Genetic susceptibility to alcohol-induced liver injury

We tested susceptibility of females from B6, CSS-17 and congenic strains (17C-1 and 17C-6) derived from CSS-17 to alcohol-induced liver injury after chronic administration of Lieber DeCarli ethanol-containing diet. No differences in daily food intake were found in all of the strains (Table 1). To ensure that the various strains metabolized ethanol in a similar manner, blood alcohol levels were measured 2hr into the feeding cycle. A/J mice had a greater increase in plasma ethanol concentrations, while all of the other strains showed similar increased plasma ethanol concentrations compared to B6 mice (Table 1). Because ethanol consumption induces CYP2E1 expression and activity (Morimoto et al., 1995), we measured the expression of CYP2E1 with Western Blot analysis. All strains had increased expression of CYP2E1 with ethanol feeding (Figure 2). Therefore, these results indicate that the genetic strains had similar increase in CYP2E1 expression, thereby validating these strains for testing of hepatic responses to perturbations.

Liver injury was characterized as an increase in hepatic triglyceride and an increase in plasma ALT after ethanol consumption compared to pair-fed controls (Dooley and ten Dijke, 2012). At the end of the alcohol-diet study, minimal hepatic lipid accumulation was detected in the A/J strain, whereas a similar increase in hepatic triglycerides was found in B6, CSS-17, 17C-1 and 17C-6 strains (Figure 3). Plasma ALTs were measured after feeding

of Lieber-DeCarli ethanol-containing diet and these values were compared to their pair-fed controls (Figure 3). A significant increase in ALTs were found in all strains. Congenic strain, 17C-1, showed the greatest increase in ALTs (3.3 fold) over its pair-fed control, while congenic strain 17C-6 had reduced ALTs compared to B6 mice. This suggested that the 17C-1 strain contains A/J allele(s) that result in increased susceptibility to alcohol-induced liver injury and 17C-6 strain contains A/J allele(s) that protect against alcohol-induced liver injury.

Genetic susceptibility to liver fibrosis

Frank fibrosis is difficult to induce with alcohol feeding alone. Therefore to identify genes modulating development of liver fibrosis, we analyzed B6, A/J, CSS-17, 17C-1, and 17C-6 using the established CCl_4 protocol (Constandinou et al., 2005). Toxicity results from the bioactivation of the CCl_4 molecule to the trichloromethyl free radical by cytochrome P450 isozymes (P450s) in the endoplasmic reticulum (Recknagel et al., 1989), specifically cytochrome P450 2E1 (CYP2E1) (Wong et al., 1998). To determine whether metabolism of CCl_4 was comparable in each strain, we measured CYP2E1 protein levels in olive oil and CCl_4 treated mice (Figure 4). All four strains had similar CYP2E1 expression levels with olive oil and they had reduced expression after CCl_4 administration, thus supporting comparable metabolism of CCl_4. The 17C-1 strain had dramatically reduced CYP2E1 expression compared to B6 (Figure 4). However in the alcohol study, 17C-1 strain had similar expression levels of CYP2E1 with alcohol consumption compared to B6 mice, suggesting that CCl_4 administration may cause more injury than alcohol consumption in the 17C-1 strain.

HSCs represent ~15% of the total cells in the liver and are located within the space of Disse. Activated HSCs show profound phenotypic changes, including enhanced cell proliferation, *de novo* expression of α-SMA and overproduction of the ECM (Lee et al., 2004). To determine whether mice developed fibrosis, liver sections from these animals were taken three days after the final CCl_4 injection, when peak fibrosis is evident (Higashiyama et al., 2007), and they were stained with Sirius red to detect extracellular matrix (ECM). Images of the stained livers were scanned and quantified. B6 and 17C-1 mice showed a moderate degree of Sirius red staining, whereas A/J, CSS-17 and 17C-6 mice had noticeably reduced Sirius red staining (Figure 5). The control olive oil injections showed no liver injury (images not shown). The livers of B6, A/J, CSS-17, 17C-1, and 17C-6 mice were also analyzed by immunohistochemistry (IHC) with α-SMA antibody and the images were scanned and quantified as described in methods. We found that B6 mice showed a moderate degree of α-SMA expression, whereas A/J, CSS-17 and 17C-6 mice had noticeably reduced α-SMA expression and 17C-1 strain had significantly more α-SMA expression (Figure 6). α-SMA protein expression was also measured by Western Blot analysis. Congenic strain, 17C-6, had 50% less α-SMA protein expression compared to B6 CCl_4 treated mice, whereas 17C-1 had 87% more expression (Figure 7). These results suggest that a small region of the A/J chromosome in congenic strain 17C-6 contains one or more genes that protect against liver fibrosis. Conversely, 17C-1 contains at least one gene that results in increased susceptibility to liver fibrosis.

Candidate genes for development of ASH

Previously we deep-sequenced DNA from the B6 and CSS-17 strains (Sudbery et al., 2009). We identified candidate genes in *Obrq 13* and *Obrq 15* that contained non-consensus SNPs in 5' untranslated region (UTR) or within the gene. The candidate genes were plasminogen (*Plg*), solute carrier family 5 (choline transporter), member 7 (*Slc5a7*), fibronectin type III domain containing 1 (*Fndc1*), and NADPH oxidase organizer 1 (*Noxo1*) for 17C-1 (*Obrq13)*, and DEAD/H (Asp-Glu-Ala-Asp/His) box helicase 11 (*Ddx11*), thyroid hormone

receptor interactor 10 (*Trip10*), cyclin-dependent kinase-like (*Cdkl4*) and NLR family, domain containing 4 (*Nlrc4*) for congenic 17C-6 (*Obrq15*) (Table 2). *Plg, Fndc1, Slc5a7, Noxo1, Ddx11, Trip10, Cdkl4* and *Nlrc4* mRNA expression was measured in livers from B6, A/J, CSS-17, 17C-1 and 17C-6 mice at the end of the treatment protocols. Although there was no statistical differences in mRNA expression for *Plg*, *Ddx11*, *Trip10* and *Cdkl4*, we did find increased *Fndc1* expression in 17C-1 ethanol fed mice and 17C-6 pair-fed mice. *Slc5a7* was significantly reduced in ethanol fed 17C-6 mice (Supplemental data figure 1). While these genes had altered expression they did not correlate with treatment. We detected altered expression for *Noxo1* and *Nlrc4* that was due to both genetics and experimental treatment. After administering the Lieber DeCarli ethanol-containing diet, increased expression of *Noxo1* was found in mice with the A/J allele for *Noxo1* (Figure 8A). Whereas increased *Nlrc4* expression was found in both pair-fed and ethanol fed strains that contained the A/J allele for *Nlrc4* (Figure 8C).To determine if these changes in gene expression also occur during fibrosis, expression of *Noxo1* and *Nlrc4* was analyzed after CCl_4 treatment (Figure 8B and 8D respectively). The congenic strain, 17C-1 which had increased liver injury also showed increased *Noxo1* expression after CCl_4 administration (Figure 8D), whereas 17C-6 had increased expression of *Nlrc4* after CCl_4 administration.

Cell specific expression and function of altered expression for Noxo1 and Nlrc4

In figure 8 the expression data were from a whole liver homogenates and thus contained all of the cell types in the liver (hepatocyte, Kupffer cells, NK cells endothelial cells and HSC). To determine if the SNPs in the A/J allele for these genes modulates expression in a cell specific manner, we isolated hepatocytes, thioglycollate-elicited peritoneal macrophages and HSC from B6, 17C-1 and 17C-6 mice fed normal CHOW diet. In the mice containing the A/J allele for *Noxo1*, the SNPs did not alter mRNA expression in isolated hepatocytes. However, *Noxo1* mRNA expression was significantly increased in isolated macrophages treated with and without LPS compared to B6 macrophages (Figure 9). *Noxo1* mRNA expression in cultured bone marrow derived macrophages (BMDM) (Supplementary data, figure 2) was also measured and showed a 10-fold increase in expression. In addition, the mRNA expression of *Noxo1* was significantly increased in HSC at day 0 compared to B6 HSC. To determine if an increase in *Noxo1* expression correlates with an increase in oxidative stress, we measured cellular ROS in BMDM from B6, CSS-17 and 17C-1 mice. The 17C-1 strain had dramatically increased ROS compared to B6 BMDM. Thus, we conclude that the SNPs in the A/J allele for the *Noxo1* gene increase *Noxo1* expression in macrophages and HSC and result in increased cellular oxidative stress which may contribute to increased fibrosis in 17C-1 mice.

In the mice containing the A/J allele for *Nlrc4*, SNPs did not alter expression in the isolated hepatocytes (Figure 10). In HSC, *Nlrc4* mRNA expression was reduced compared to B6 HSC. However, *Nlrc4* expression was significantly increased in isolated thioglycollate-elicited peritoneal macrophages treated with and without LPS compared to B6 macrophages. Since *Nlrc4* is part of the inflammasome, we wanted to determine if increased *Nlrc4* expression correlated with increased inflammation. Therefore, neutrophil infiltration was measured with an antibody for NIMP-R14 in liver sections from B6 and 17C-6 mice. There was an increase of NIMP-R14 positive cells in 17C-6 strain compared to B6 and CSS-17 mice. As a result, we conclude that the SNPs in the A/J allele for the *Nlrc4* gene increased *Nlrc4* expression in macrophages and result in increased hepatic inflammation in the 17C-6 strain.

Discussion

The aim of the present study was to identify novel candidate genes involved in development of liver injury and fibrosis. B6, A/J, CSS-17 and 17C-1 and 17C-6 congenic strains were

analyzed for hepatic steatosis and liver injury in response to chronic alcohol feeding or administration of CCl_4. We hypothesized that because progression of liver disease from steatosis to cirrhosis is similar for patients with ASH and NASH, the genes and pathways that were previously identified on a high fat diet would be similar for alcohol consumption and CCl_4 treatment. However, we found that *Obrq13* promoted liver injury and fibrosis, and *Obrq15* protected mice from alcohol-induced liver injury and fibrosis. Therefore genetics, and the molecular mechanisms for progression to ASH and NASH, appear to have distinctive features (Table 2).

By using the congenic strains derived from CSS-17, the consequences of a very small region of the A/J chromosome 17 in context of the B6 chromosome was studied. This illustrates one of many advantages in using CSS strains and congenics strains over a traditional F1 cross between B6 and A/J inbred strains. The isogenic A/J chromosome in CSSs enables us to: 1) identify both dominant and recessive genes modulating liver injury, 2) maintain a genetically identical mouse strain for continued functional and mechanistic studies, and 3) decouple phenotypes to investigate their independent contributions to disease. With the CSS paradigm several candidate genes that were located in either *Obrq13 (Fndc1, Plg, Slc5a7 and Noxo1)* or *Obrq15 (Trip 10, Ddx11, Cdkl4 and Nlrc4)* were identified. Little is known about the role of these genes in the liver. *Fndc1* has been found to be elevated in patients with skin tumors (Anderegg et al., 2005). Increased choline transporter expression and activity from *Slc5a7* has been found in patients with Alzheimer's disease (Bissette et al., 1996). In the supplementary data figure 1, the expression of these genes was not altered between strains except for *Fndc1* and *Slc5a7*. The role of these genes in the development of liver disease is not clear and requires more analysis. In this study, we focused on the two candidate genes that had altered gene expression due to genetic variance and experimental treatments.

Patients with chronic liver injury from alcohol or hepatitis C viral infection have increased ROS and oxidative stress (Parola and Robino, 2001). In the hepatocyte, ROS is generated from CYP2E1 activation with alcohol consumption and the apoptotic bodies from damaged hepatocyte can activate quiescent HSC to become activated HSC that produce collagen and proliferate. ROS can also be produced by plasma membrane-associated NADPH oxidase (Babior et al., 2002). In the resident macrophage of the liver, Kupffer cells, NADPH oxidase reduces molecular oxygen to generate superoxide which is converted to hydrogen peroxide (Babior et al., 2002). The activation of oxidants increase redox-sensitive transcription factor, nuclear factor kappa-light-chain-enhancer of activated B cells (NFκB), and increases expression of critical cytokines, such as tumor necrosis factor α (TNFα) and interleukins. These cytokines activate a signaling cascade in the hepatocyte and ultimately cause apoptosis and can activate the HSC (Wheeler et al., 2001).

Using the CSS paradigm, we identified two candidate genes, *Noxo1* and *Nlrc4*, that modulate liver injury. Identification of *Noxo1* supports published evidence that the NOX family of NADPH oxidases contributes to liver disease (Bataller et al., 2003). This gene family of proteins transfers electrons across biological membranes and the product of the electron transfer reaction is superoxide (Ushio-Fukai, 2006).

The NADPH oxidase is a multi-subunit enzyme that has catalytic subunits as well as regulator subunits called "organizer subunits" (Bedard and Krause, 2007). NADPH oxidase activity is controlled by regulatory subunits including Nox regulators $p47^{phox}$, $p67^{phox}$ and their homolog's *Noxo1* (our gene of interest), *NoxA1* or *Duox1A1* or *Duoax2.* The impact that these regulatory subunits have on modulating NADPH oxidase activity has been minimally studied. One study showed mice that deficient for $p47^{phox}$ ($p47^{phox-/-}$) are resistant to chronic ethanol-induced liver injury (Kono et al., 2000).

In this study, we show that increased expression of regulatory subunit, *Noxo1*, in BMDM isolated from 17C-6 resulted in greater cellular ROS. We propose that the SNPs in the A/J allele of *Noxo1* increase gene expression of the regulator, *Noxo1*, thus increasing the activity of NADPH oxidase. This in turn would generate more oxidative stress in macrophages and activate HSC resulting in greater fibrosis for the 17C-1 strain. There may also be cross-talk between the macrophage, HSC and hepatocytes that were not detected in our primary cultured cells. Future studies will analyze altered expression of *Noxo1* in co-culture experiments to determine the impact of altered macrophage expression of *Noxo1* and NADPH oxidase on HSC function.

The second gene we identified was *Nlrc4* which supported a role for the immune system in development of liver fibrosis. Presently the current hypothesis for ethanol-induced liver injury proposes that ethanol consumption may result in leakage of bacterial products from the gut, altering the jejunal microflora and leading to proliferation of gram-negative bacteria. LPS, a component of the cell wall in gram negative bacteria, is increased in circulation of alcoholics (Wang et al., 2010). The increased LPS induces TNFα production from Kupffer cells. In addition recognition of conserved microbial structures known as pathogen associated molecular patterns (PAMP) is accomplished by membrane bound Toll-like receptors (TLRs) and cytoplasmic nucleotide oligomerization domain like receptors (NLRs) (Schroder and Tschopp, 2010). Upon sensing of PAMPs, NLRs interact with members of the inflammasome complex, and the aassembly of the inflammasome complex leads to cleavage and activation of procaspase-1 (Schroder and Tschopp, 2010). Once activated, caspase-1 promotes proteolytic maturation and activation of IL-1β, IL-18 and caspase-7 and deactivation of IL-33 (Lamkanfi et al., 2007) as well as mediating apoptotic cell death (Bergsbaken et al., 2009).

Nlrc4 mRNA was elevated in isolated macrophage, yet it was decreased in isolated HSC (day 0 and day 7 of culture) from 17C-6 mice (Figure 10). This increased expression of *Nlrc4* was associated with induced inflammation as measured by infiltration of neutrophils recognized with NIMP-R14 IHC. We propose that the increase of *Nlrc4* in the macrophage and decrease of *Nlrc4* mRNA expression in the HSC are protective from CCl_4 induced fibrosis. The mechanism is not understood, but we hypothesize that increased *Nlrc4* expression induces Nlrc4 inflammasome activity. This in turn would increase activation of caspase-1 activity, and release of cytokines, IL-1β and IL-18. IL-18 has been shown to induce expression of interferon γ (IFN-γ) in macrophages (Barbulescu et al., 1998; Baroni et al., 1996; Nakahira et al., 2002). Previous studies found that IFN-γ administration to HSC inhibits *in vitro* activation of HSC and caused a marked decrease in collagen synthesis (Czaja et al., 1987). IFN-α has also been shown to inhibit proliferation of HSC and induce apoptosis of HSC (Ogawa et al., 2009). Another potential mechanism could be a direct effect on hepatocyte regeneration via IL-18 and IL-6. Studies in mice reveal that IL-18 stimulation of peritoneal macrophages induces IL-6 production (Netea et al., 2000). We suggest that the increased of *Nlrc4* expression in the macrophage would increase IL-18, which in turn could increase IL-6 production. IL-6 can bind to its receptor in the hepatocyte and initiate a signaling cascade that would promote liver regeneration (Taub, 2004). Future studies will look at the cross-talk between macrophage and hepatocytes and will be used to understand the mechanism for protection from liver injury by *Nlrc4*.

In summary we found altered gene expression of the A/J-derived alleles for *Noxo1* and *Nlrc4* compared to B6 alleles. We suggest that sequence differences in regulatory or coding regions of these genes modulate development, maintenance, and resolution of fibrosis. Future studies will address these issues using congenic strains and knockout animals for each gene and analyze the role of these genes within Kupffer cells, HSC, and hepatocytes and the cross-talk between these cells. Elucidation of the molecular mechanisms behind

these genes will improve our fundamental knowledge of the mechanism(s) for progression to fibrosis and will promote the development of new therapeutic interventions to prevent ASH.

Supplementary Material

Refer to Web version on PubMed Central for supplementary material.

References

Anderegg U, Breitschwerdt K, Kohler MJ, Sticherling M, Haustein UF, Simon JC, Saalbach A. MEL4B3, a novel mRNA is induced in skin tumors and regulated by TGF-beta and pro-inflammatory cytokines. Exp Dermatol. 2005; 14:709–718. [PubMed: 16098131]

Babior BM, Lambeth JD, Nauseef W. The neutrophil NADPH oxidase. Arch Biochem Biophys. 2002; 397:342–344. [PubMed: 11795892]

Barbulescu K, Becker C, Schlaak JF, Schmitt E, Meyer zum Buschenfelde KH, Neurath MF. IL-12 and IL-18 differentially regulate the transcriptional activity of the human IFN-gamma promoter in primary CD4+ T lymphocytes. J Immunol. 1998; 160:3642–3647. [PubMed: 9558063]

Baroni GS, D'Ambrosio L, Curto P, Casini A, Mancini R, Jezequel AM, Benedetti A. Interferon gamma decreases hepatic stellate cell activation and extracellular matrix deposition in rat liver fibrosis. Hepatology. 1996; 23:1189–1199. [PubMed: 8621153]

Bataller R, Schwabe RF, Choi YH, Yang L, Paik YH, Lindquist J, Qian T, Schoonhoven R, Hagedorn CH, Lemasters JJ, Brenner DA. NADPH oxidase signal transduces angiotensin II in hepatic stellate cells and is critical in hepatic fibrosis. J Clin Invest. 2003; 112:1383–1394. [PubMed: 14597764]

Bedard K, Krause KH. The NOX family of ROS-generating NADPH oxidases: physiology and pathophysiology. Physiol Rev. 2007; 87:245–313. [PubMed: 17237347]

Bergsbaken T, Fink SL, Cookson BT. Pyroptosis: host cell death and inflammation. Nat Rev Microbiol. 2009; 7:99–109. [PubMed: 19148178]

Bissette G, Seidler FJ, Nemeroff CB, Slotkin TA. High affinity choline transporter status in Alzheimer's disease tissue from rapid autopsy. Ann N Y Acad Sci. 1996; 777:197–204. [PubMed: 8624084]

Blomhoff R, Berg T. Isolation and cultivation of rat liver stellate cells. Methods Enzymol. 1990; 190:58–71. [PubMed: 1965004]

Buchner DA, Burrage LC, Hill AE, Yazbek SN, O'Brien WE, Croniger CM, Nadeau JH. Resistance to diet-induced obesity in mice with a single substituted chromosome. Physiol Genomics. 2008; 35:116–122. [PubMed: 18628339]

Constandinou C, Henderson N, Iredale JP. Modeling liver fibrosis in rodents. Methods Mol Med. 2005; 117:237–250. [PubMed: 16118456]

Czaja MJ, Weiner FR, Eghbali M, Giambrone MA, Zern MA. Differential effects of gamma-interferon on collagen and fibronectin gene expression. J Biol Chem. 1987; 262:13348–13351. [PubMed: 3115979]

Diehl AM, Goodman Z, Ishak KG. Alcohollike liver disease in nonalcoholics. A clinical and histologic comparison with alcohol-induced liver injury. Gastroenterology. 1988; 95:1056–1062. [PubMed: 3410220]

Dooley S, ten Dijke P. TGF-beta in progression of liver disease. Cell Tissue Res. 2012; 347:245–256. [PubMed: 22006249]

Edenberg HJ, Xuei X, Chen HJ, Tian H, Wetherill LF, Dick DM, Almasy L, Bierut L, Bucholz KK, Goate A, Hesselbrock V, Kuperman S, Nurnberger J, Porjesz B, Rice J, Schuckit M, Tischfield J, Begleiter H, Foroud T. Association of alcohol dehydrogenase genes with alcohol dependence: a comprehensive analysis. Hum Mol Genet. 2006; 15:1539–1549. [PubMed: 16571603]

Gines P, Cardenas A, Arroyo V, Rodes J. Management of cirrhosis and ascites. N Engl J Med. 2004; 350:1646–1654. [PubMed: 15084697]

Higashiyama R, Inagaki Y, Hong YY, Kushida M, Nakao S, Niioka M, Watanabe T, Okano H, Matsuzaki Y, Shiota G, Okazaki I. Bone marrow-derived cells express matrix metalloproteinases

and contribute to regression of liver fibrosis in mice. Hepatology. 2007; 45:213–222. [PubMed: 17187438]

Hong J, Stubbins RE, Smith RR, Harvey AE, Nunez NP. Differential susceptibility to obesity between male, female and ovariectomized female mice. Nutr J. 2009; 8:11. [PubMed: 19220919]

Itoga S, Harada S, Nomura F. Polymorphism of the 5'-flanking region of the CYP2E1 gene: an association study with alcoholism. Alcohol Clin Exp Res. 2001; 25:11S–15S. [PubMed: 11410734]

Kimura M, Higuchi S. Genetics of alcohol dependence. Psychiatry Clin Neurosci. 2011; 65:213–225. [PubMed: 21507127]

Kono H, Rusyn I, Yin M, Gabele E, Yamashina S, Dikalova A, Kadiiska MB, Connor HD, Mason RP, Segal BH, Bradford BU, Holland SM, Thurman RG. NADPH oxidase-derived free radicals are key oxidants in alcohol-induced liver disease. J Clin Invest. 2000; 106:867–872. [PubMed: 11018074]

Lamkanfi M, Kanneganti TD, Franchi L, Nunez G. Caspase-1 inflammasomes in infection and inflammation. J Leukoc Biol. 2007; 82:220–225. [PubMed: 17442855]

Lee SH, Chae KS, Sohn DH. Identification of expressed sequence tags of genes expressed highly in the activated hepatic stellate cell. Arch Pharm Res. 2004; 27:422–428. [PubMed: 15180308]

Lin P, Hartz SM, Wang JC, Agrawal A, Zhang TX, McKenna N, Bucholz K, Brooks AI, Tischfield JA, Edenberg HJ, Hesselbrock VM, Kramer JR, Kuperman S, Schuckit MA, Goate AM, Bierut LJ, Rice JP. Copy Number Variations in 6q14.1 and 5q13.2 are Associated with Alcohol Dependence. Alcohol Clin Exp Res. 2012; 36:1512–1518. [PubMed: 22702843]

Millward CA, Burrage LC, Shao H, Sinasac DS, Kawasoe JH, Hill-Baskin AE, Ernest SR, Gornicka A, Hsieh CW, Pisano S, Nadeau JH, Croniger CM. Genetic factors for resistance to diet-induced obesity and associated metabolic traits on mouse chromosome 17. Mamm Genome. 2009; 20:71–82. [PubMed: 19137372]

Millward CA, Desantis D, Hsieh CW, Heaney JD, Pisano S, Olswang Y, Reshef L, Beidelschies M, Puchowicz M, Croniger CM. Phosphoenolpyruvate carboxykinase (Pck1) helps regulate the triglyceride/fatty acid cycle and development of insulin resistance in mice. J Lipid Res. 2010; 51:1452–1463. [PubMed: 20124556]

Morimoto M, Hagbjork AL, Wan YJ, Fu PC, Clot P, Albano E, Ingelman-Sundberg M, French SW. Modulation of experimental alcohol-induced liver disease by cytochrome P450 2E1 inhibitors. Hepatology. 1995; 21:1610–1617. [PubMed: 7768506]

Nakahira M, Ahn HJ, Park WR, Gao P, Tomura M, Park CS, Hamaoka T, Ohta T, Kurimoto M, Fujiwara H. Synergy of IL-12 and IL-18 for IFN-gamma gene expression: IL-12-induced STAT4 contributes to IFN-gamma promoter activation by up-regulating the binding activity of IL-18-induced activator protein 1. J Immunol. 2002; 168:1146–1153. [PubMed: 11801649]

Netea MG, Kullberg BJ, Verschueren I, Van Der Meer JW. Interleukin-18 induces production of proinflammatory cytokines in mice: no intermediate role for the cytokines of the tumor necrosis factor family and interleukin-1beta. Eur J Immunol. 2000; 30:3057–3060. [PubMed: 11069090]

Ogawa T, Kawada N, Ikeda K. Effect of natural interferon alpha on proliferation and apoptosis of hepatic stellate cells. Hepatol Int. 2009; 3:497–503. [PubMed: 19669254]

Parola M, Robino G. Oxidative stress-related molecules and liver fibrosis. J Hepatol. 2001; 35:297–306. [PubMed: 11580156]

Pritchard MT, Malinak RN, Nagy LE. Early growth response (EGR)-1 is required for timely cell-cycle entry and progression in hepatocytes after acute carbon tetrachloride exposure in mice. Am J Physiol Gastrointest Liver Physiol. 2011; 300:G1124–G1131. [PubMed: 21415413]

Pritchard MT, Nagy LE. Hepatic fibrosis is enhanced and accompanied by robust oval cell activation after chronic carbon tetrachloride administration to Egr-1-deficient mice. Am J Pathol. 2010; 176:2743–2752. [PubMed: 20395449]

Recknagel RO, Glende EA Jr, Dolak JA, Waller RL. Mechanisms of carbon tetrachloride toxicity. Pharmacol Ther. 1989; 43:139–154. [PubMed: 2675128]

Salmon DM, Flatt JP. Effect of dietary fat content on the incidence of obesity among ad libitum fed mice. Int J Obes. 1985; 9:443–449. [PubMed: 3830936]

Sato N, Lindros KO, Baraona E, Ikejima K, Mezey E, Jarvelainen HA, Ramchandani VA. Sex difference in alcohol-related organ injury. Alcohol Clin Exp Res. 2001; 25:40S–45S. [PubMed: 11391047]

Schroder K, Tschopp J. The inflammasomes. Cell. 2010; 140:821–832. [PubMed: 20303873]

Singer JB, Hill AE, Burrage LC, Olszens KR, Song J, Justice M, O'Brien WE, Conti DV, Witte JS, Lander ES, Nadeau JH. Genetic dissection of complex traits with chromosome substitution strains of mice. Science. 2004; 304:445–448. [PubMed: 15031436]

Sudbery I, Stalker J, Simpson JT, Keane T, Rust AG, Hurles ME, Walter K, Lynch D, Teboul L, Brown SD, Li H, Ning Z, Nadeau JH, Croniger CM, Durbin R, Adams DJ. Deep short-read sequencing of chromosome 17 from the mouse strains A/J and CAST/Ei identifies significant germline variation and candidate genes that regulate liver triglyceride levels. Genome Biol. 2009; 10:R112. [PubMed: 19825173]

Taub R. Liver regeneration: from myth to mechanism. Nat Rev Mol Cell Biol. 2004; 5:836–847. [PubMed: 15459664]

Ushio-Fukai M. Localizing NADPH oxidase-derived ROS. Sci STKE 2006. 2006:re8.

Vasiliou V, Pappa A, Petersen DR. Role of aldehyde dehydrogenases in endogenous and xenobiotic metabolism. Chem Biol Interact. 2000; 129:1–19. [PubMed: 11154732]

Wang HJ, Zakhari S, Jung MK. Alcohol, inflammation, and gut-liver-brain interactions in tissue damage and disease development. World J Gastroenterol. 2010; 16:1304–1313. [PubMed: 20238396]

Webb A, Lind PA, Kalmijn J, Feiler HS, Smith TL, Schuckit MA, Wilhelmsen K. The investigation into CYP2E1 in relation to the level of response to alcohol through a combination of linkage and association analysis. Alcohol Clin Exp Res. 2011; 35:10–18. [PubMed: 20958328]

West MA, Billiar TR, Curran RD, Hyland BJ, Simmons RL. Evidence that rat Kupffer cells stimulate and inhibit hepatocyte protein synthesis in vitro by different mechanisms. Gastroenterology. 1989; 96:1572–1582. [PubMed: 2497043]

Wheeler MD, Kono H, Yin M, Nakagami M, Uesugi T, Arteel GE, Gabele E, Rusyn I, Yamashina S, Froh M, Adachi Y, Iimuro Y, Bradford BU, Smutney OM, Connor HD, Mason RP, Goyert SM, Peters JM, Gonzalez FJ, Samulski RJ, Thurman RG. The role of Kupffer cell oxidant production in early ethanol-induced liver disease. Free Radic Biol Med. 2001; 31:1544–1549. [PubMed: 11744328]

Wong FW, Chan WY, Lee SS. Resistance to carbon tetrachloride-induced hepatotoxicity in mice which lack CYP2E1 expression. Toxicol Appl Pharmacol. 1998; 153:109–118. [PubMed: 9875305]

Xuei X, Dick D, Flury-Wetherill L, Tian HJ, Agrawal A, Bierut L, Goate A, Bucholz K, Schuckit M, Nurnberger J Jr, Tischfield J, Kuperman S, Porjesz B, Begleiter H, Foroud T, Edenberg HJ. Association of the kappa-opioid system with alcohol dependence. Mol Psychiatry. 2006; 11:1016–1024. [PubMed: 16924269]

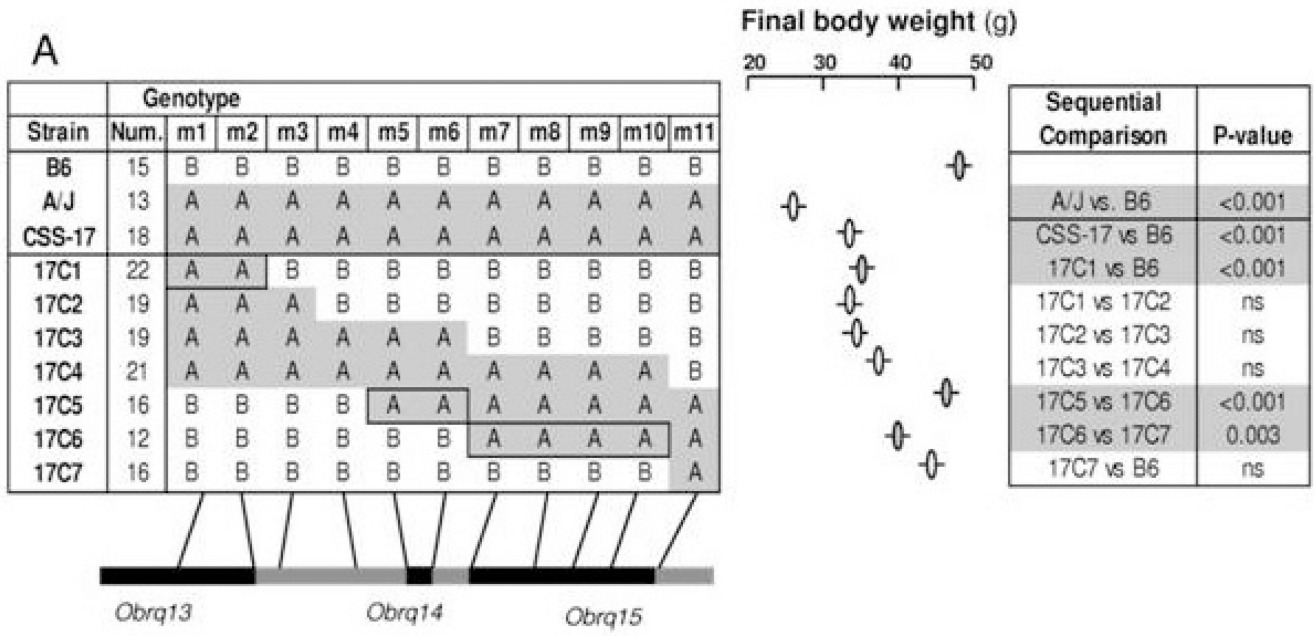

Figure 1. Congenic strains from CSS-17

A) Construction of congenics strains derived from CSS-17. A/J derived segments are represented with shaded squares and the letter “A”, and C57BL/6J-derived segments are represented with white squares and the letter “B”. Genetic markers (m1 to m11 as described) are listed in order from centromere (left) to telomere (right) (Millward et al., 2009) and are represented to scale showing their approximate location of DNA sequence obtained from the Mouse Genome Informatics website (www.informatics.jax.org). The number of mice tested in each group is in the column labeled “Num”. Chromosomal regions inferred to contain a QTL, based on strong phenotypic differences between strains, are indicated.

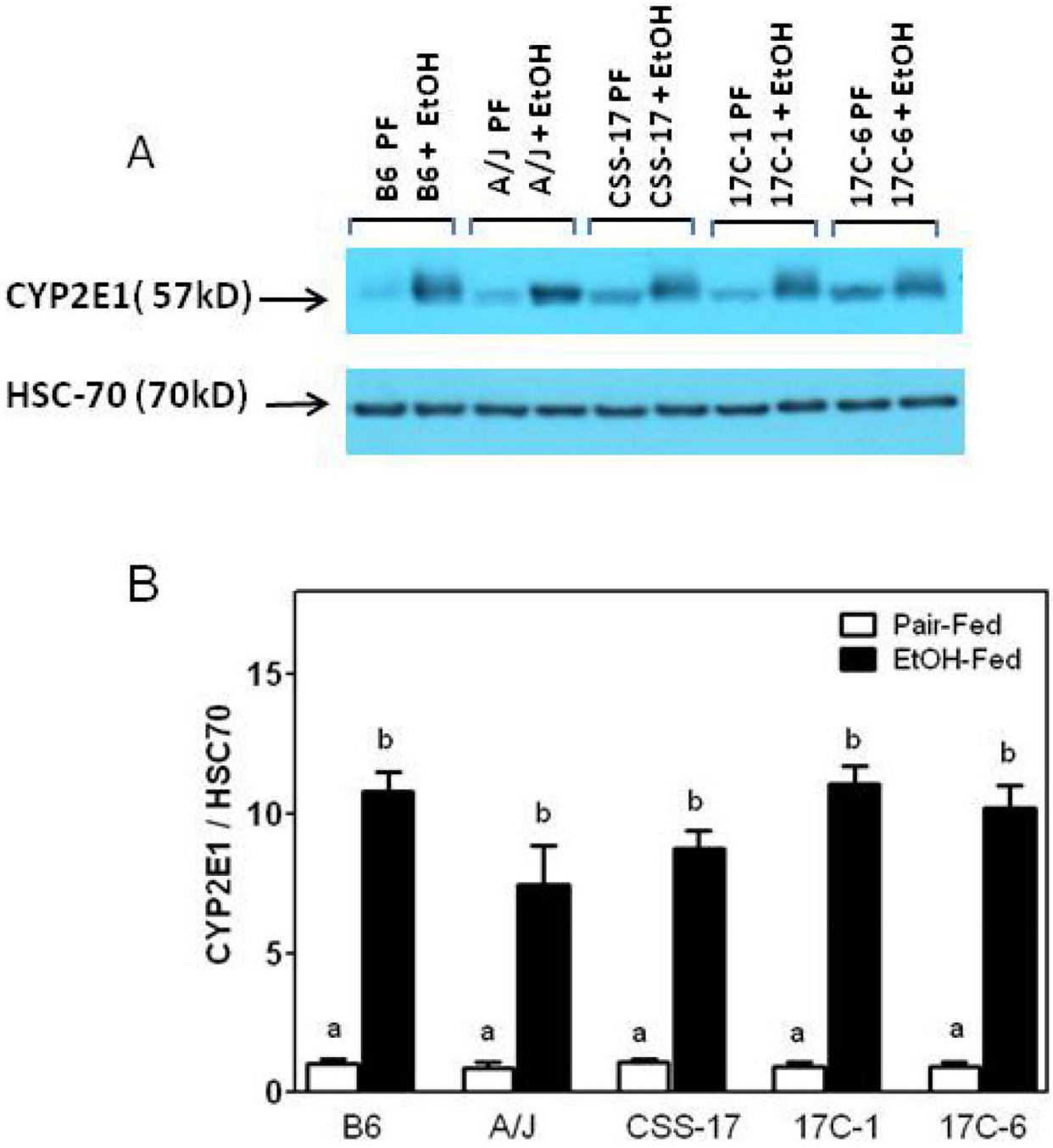

Figure 2. CYP2E1 induction with alcohol consumption

A) Western analysis of proteins from mice fed ethanol-containing diet (EtOH-fed) or pair-fed diet (Pair-fed). Westerns were normalized with HSC70 as a loading control. B) Densitometric scan of Western Blots. Values represent mean ±SEM for a total of 4–6 female mice per group. Values with different superscripts are significantly different $P<0.05$ as determined with ANOVA and Bonferroni's correction for multiple testing. Abbreviations, PF, pair-fed diet, +EtOH, Etoh-containing diet.

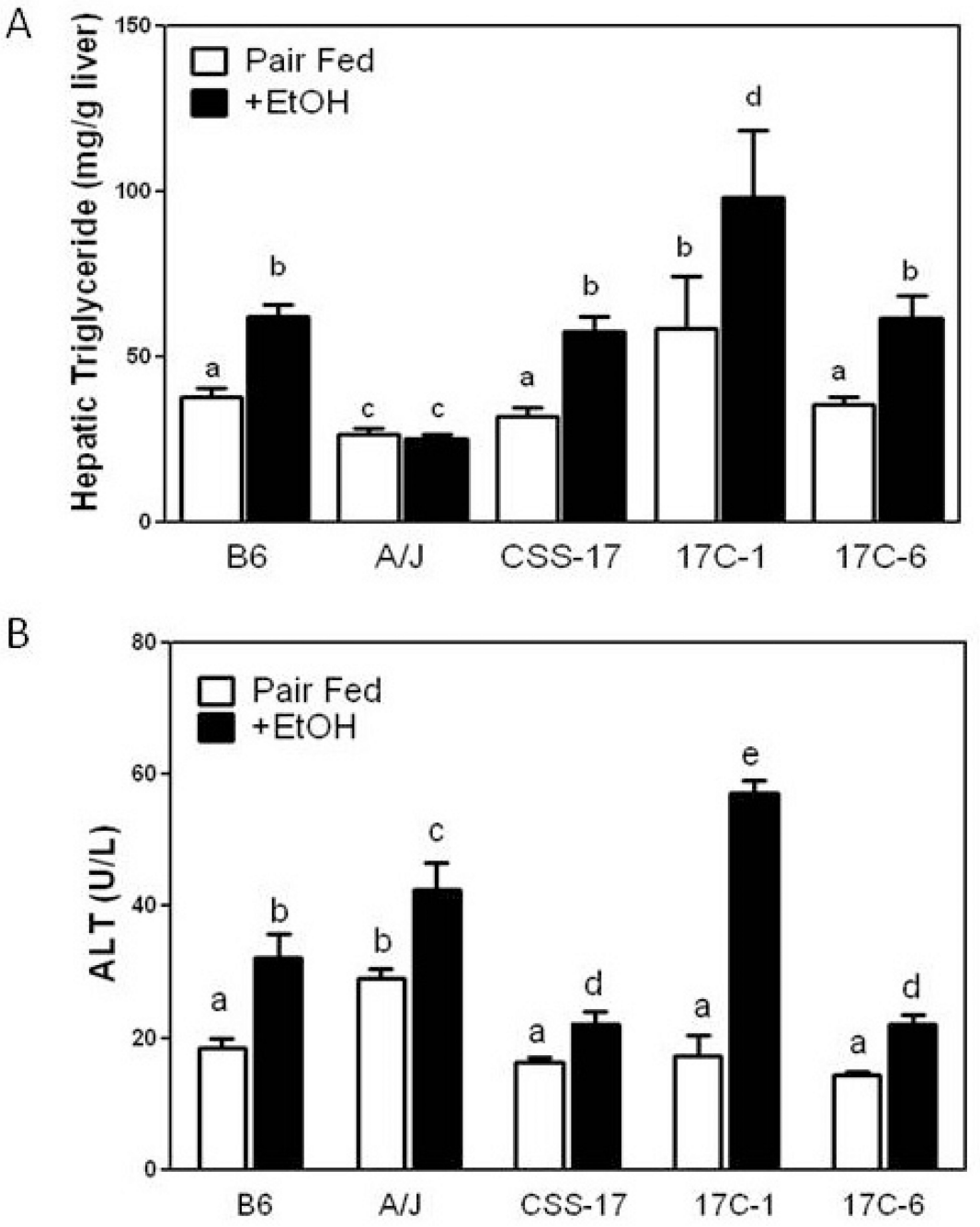

Figure 3. Measurements of liver injury

A) Hepatic triglycerides were measured biochemically from mice fed the ethanol-containing diet (EtOH-fed)) or pair-fed diet (Pair-fed). Plasma B) ALT were measured with enzymatic assays from mice at the end of the ethanol feeding trial. Values represent mean ±SEM for a total of 4–6 female mice per group. Values with different superscripts are significantly different from each other, $P<0.05$ as determined with ANOVA and Bonferroni's correction for multiple testing.

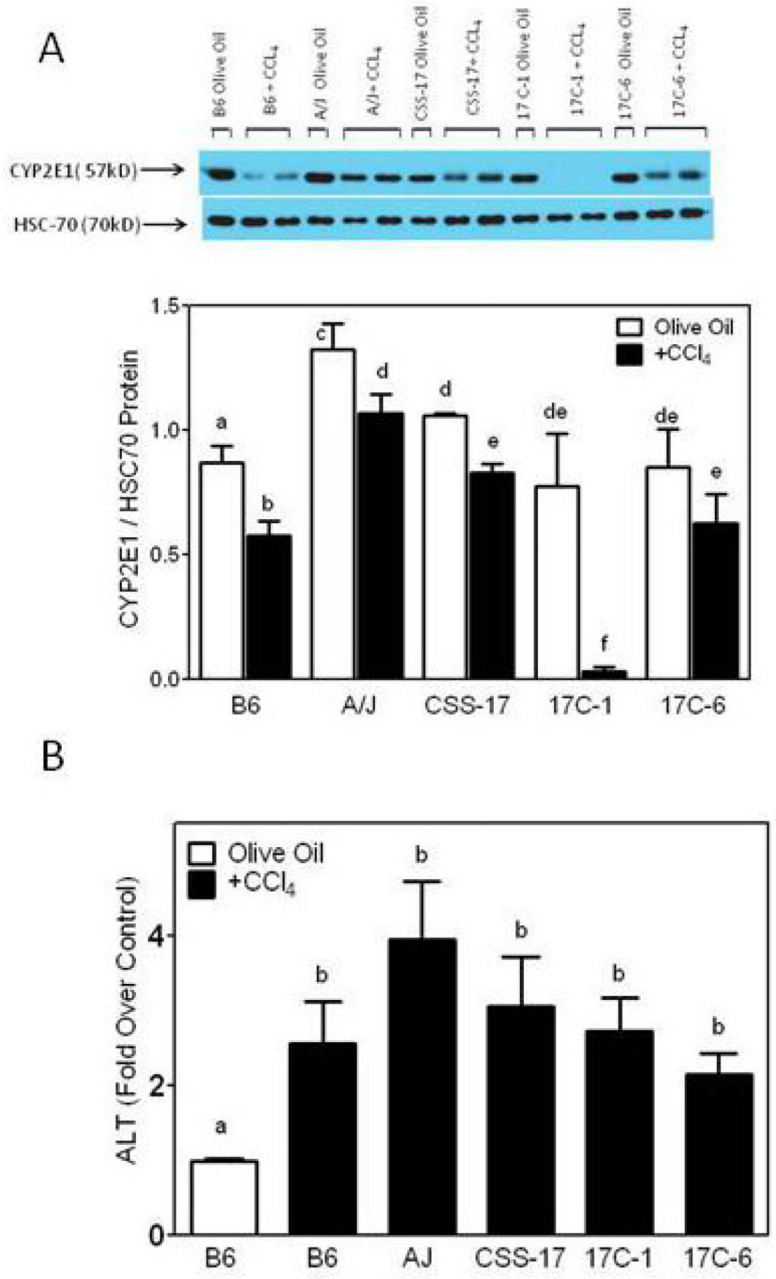

Figure 4. Response to chronic CCl_4 administration in congenic strains

A) Western analysis of hepatic proteins from mice treated with CCl_4 as described in Methods. Western blots were normalized with HSC70 as a loading control. Densitometric scanning of Western Blots are shown. B) Plasma ALT measurement of mice 3 days after the final CCl_4 dose. Values represent mean ±SEM for a total of 6–10 male mice per group. Values with different superscripts are significantly different from each other, $P<0.05$ as determined with ANOVA and Bonferroni's correction for multiple testing.

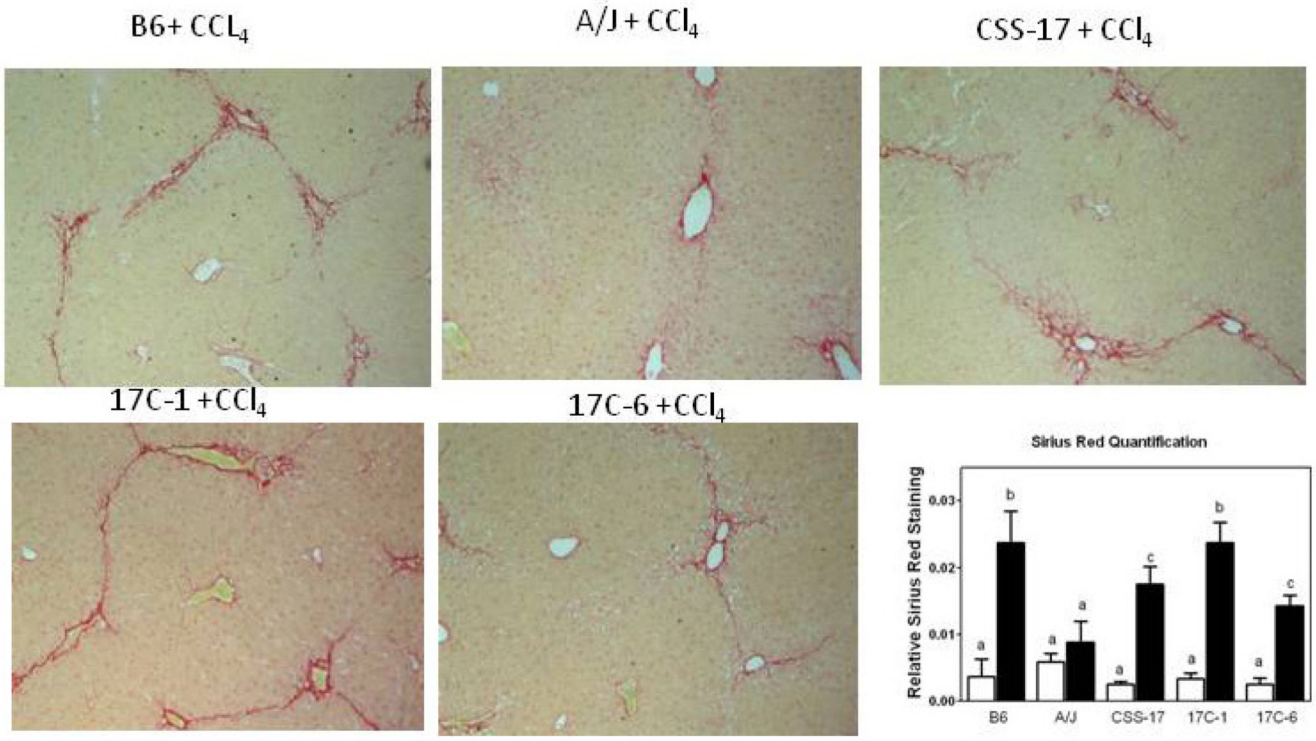

Figure 5. Reduced liver fibrosis in 17C-6 congenic strain

At 3 days after the final CCl_4 dose, mice were euthanized and livers were stained with Sirius red. Images were taken at 5× magnification. The images were scanned and quantified as described in Methods. Values are means± SEM, n=6–10 male mice per group. Superscripts without a common letter differ from each other, $P<0.05$ as determined with ANOVA and Bonferroni's correction for multiple testing.

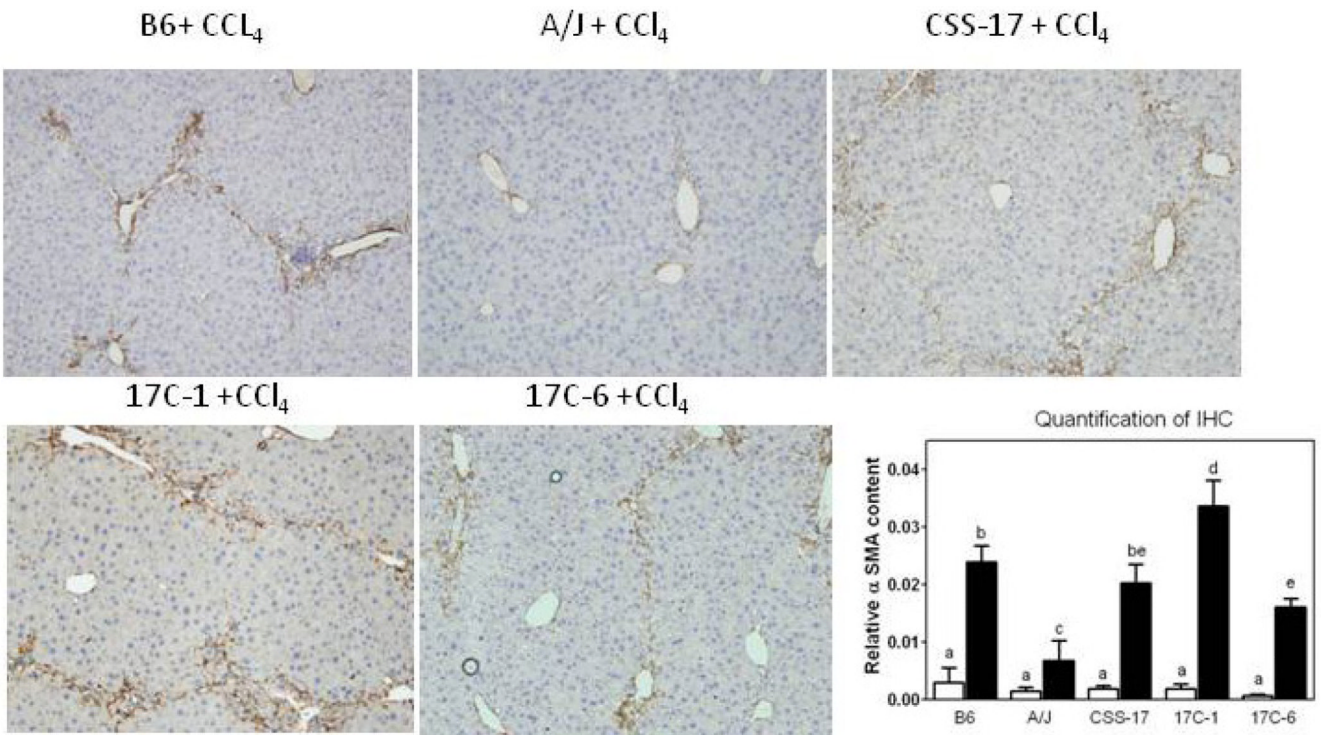

Figure 6. Immunihistochemistry with α-SMA

At 3 days after final CCl_4 injection, mice were euthanized and portions of individual livers preserved in formalin for assessment of α-SMA protein expression by immunohistochemistry. Images were taken at 10× magnification. The images were scanned and quantified as described in Methods. Values are means± SEM, n=4–10 male mice per group. Superscripts without a common letter differ from each other, $P<0.05$ as determined with ANOVA and Bonferroni's correction for multiple testing.

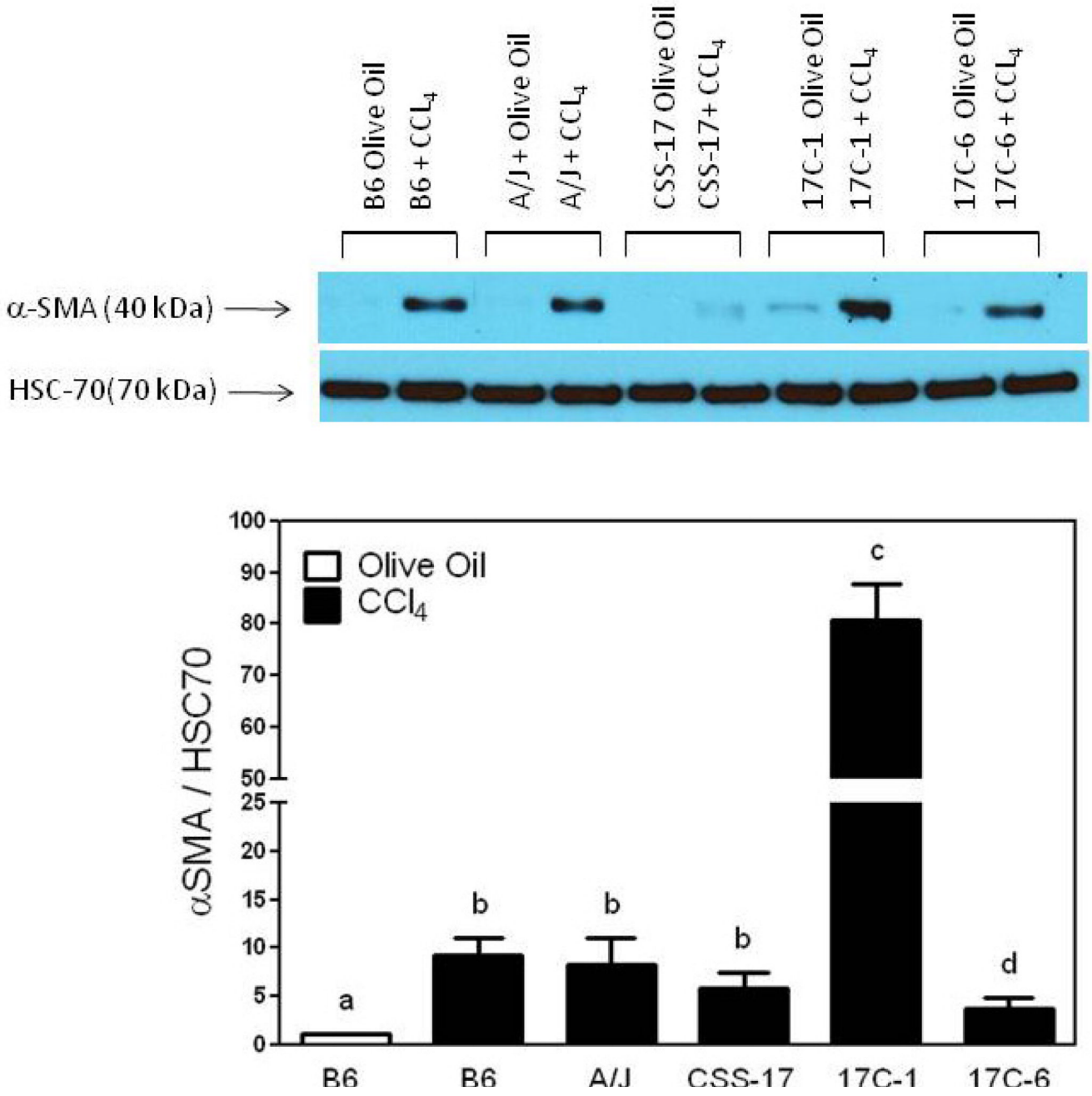

Figure 7. Detection of α-SMA

Livers from B6, CSS-17, 17C-1 and 17C-6 were treated with CCl_4 and analyzed for expression of α-SMA by A) Western Blot normalized with HSC-70 for loading control. Densitometric scans of a representative Western Blot is shown, n=4–6 male mice per group. Values with different superscripts are significantly different from each other, $P<0.05$ as determined with ANOVA Bonferroni's correction for multiple testing.

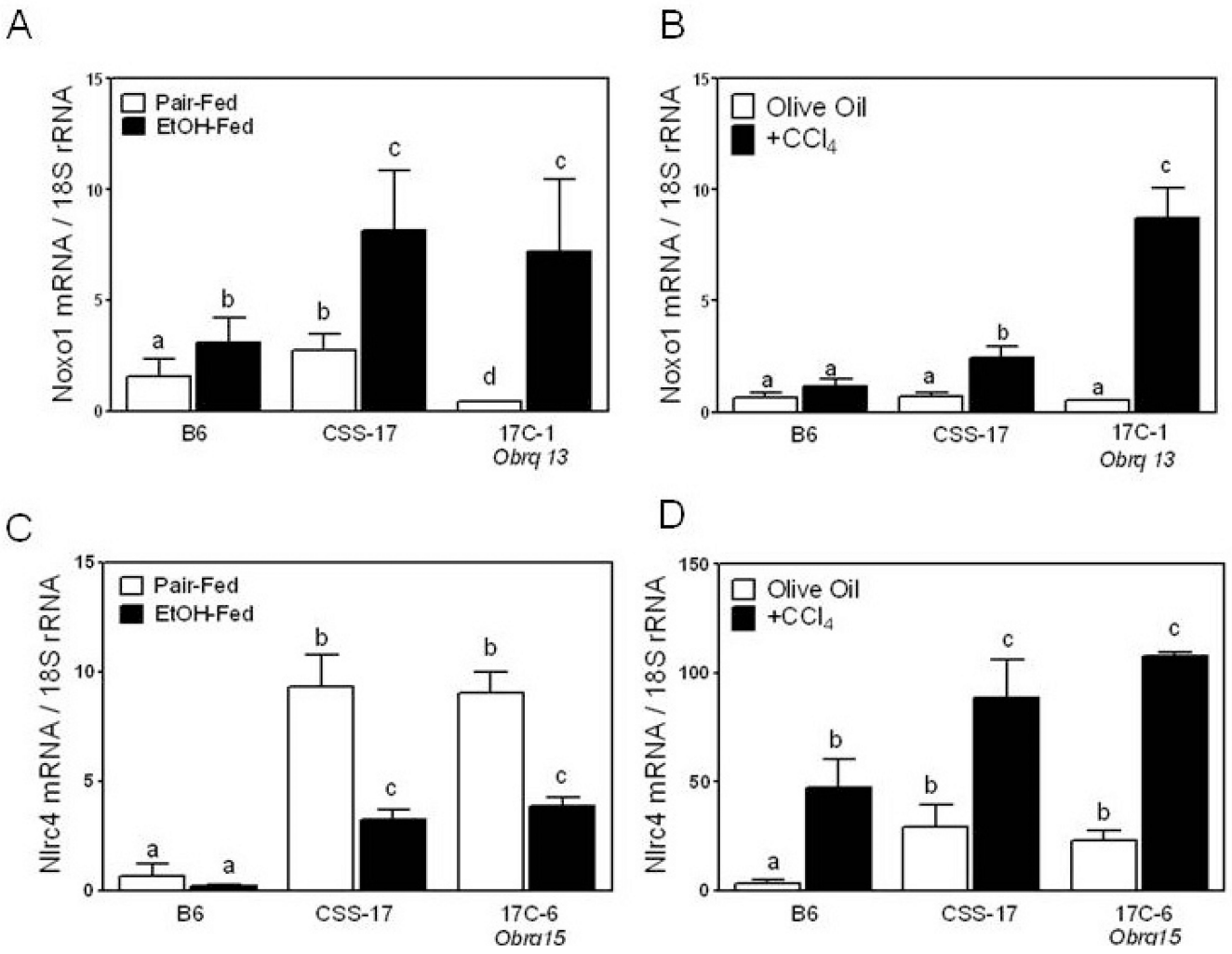

Figure 8. Expression of candidate genes in congenic strains

RNA was isolated from mice fed Lieber DeCarli ethanol-containing diet (EtOH-fed) or pair fed controls (Paire-fed) or treated with either olive oil or CCl_4 injections 2×/week for three weeks. Expression of *Noxo1* mRNA in A) ethanol-fed and pair-fed mice and B) CCl_4 treated mice. Expression of *Nlrc4* mRNA in C) ethanol-fed and pair-fed mice and D) CCl_4 treated mice. The values are the means ±SEM and normalized with 18S rRNA for n=4–6 mice per group. Superscripts without a common letter differ from each other, $P<0.05$ as determined with ANOVA and Bonferroni's correction for multiple testing.

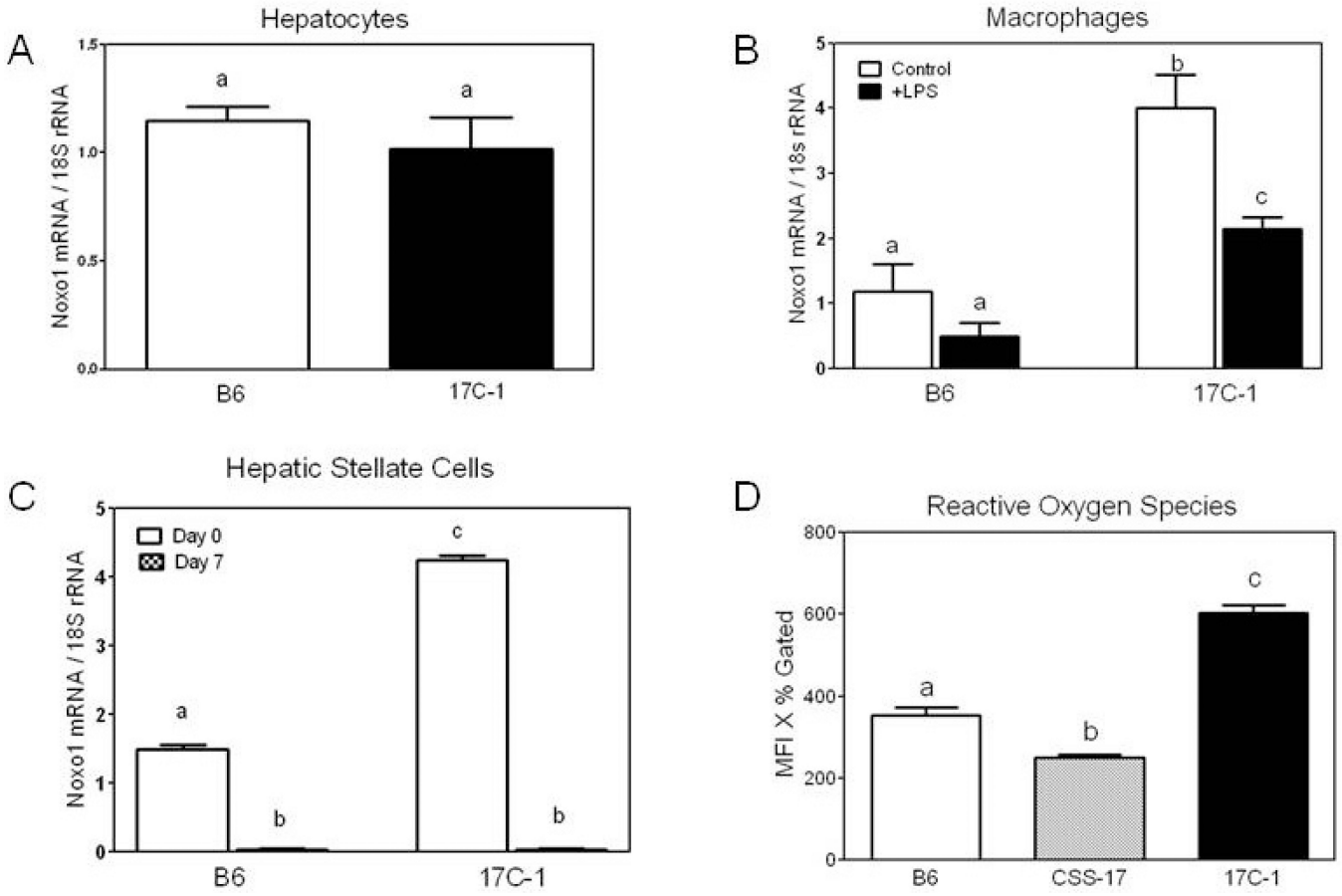

Figure 9. Expression of Noxo1 in cells isolated from the liver

Hepatocytes, macrophages and hepatic stellate cells were isolated from livers of B6 and 17C-1 mice as described in Methods. RNA was isolated from A) hepatocytes, B) macrophages with and without LPS stimulation and C) HSC on day 0 or after 7 days of culture. Expression of Noxo1 was measured by RT-PCR. The values are the means ±SEM and normalized with 18S rRNA for n=4–6 mice per group. D) Bone marrow derived macrophages were isolated from B6 and 17C-1 mice and cellular reactive oxygen species (ROS) as described in Methods. Superscripts without a common letter differ from each other, $P<0.05$ as determined with ANOVA and Bonferroni's correction for multiple testing.

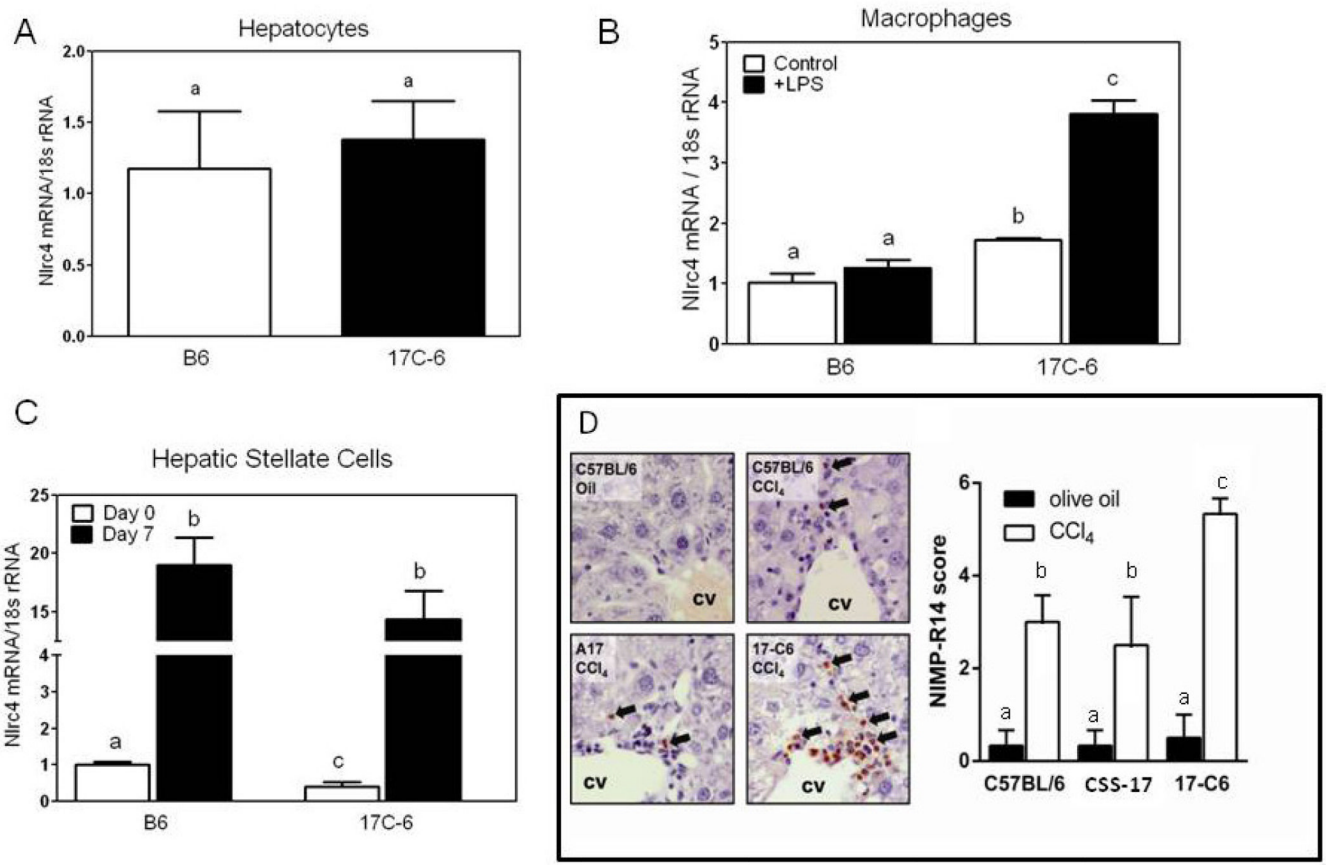

Figure 10. Expression of Nlrc4 in cells isolated from the liver

Hepatocytes, macrophages and hepatic stellate cells were isolated from livers of B6 and 17C-6 mice as described in Methods. RNA was isolated from A) hepatocytes, B) macrophages with and without LPS stimulation and C) HSC on day 0 or after 7 days of culture. Expression of Nlrc4 was measured by RT-PCR. The values are the means ±SEM and normalized with 18S rRNA for n=4–6 mice per group. Superscripts without a common letter differ from each other, $P<0.05$ as determined with ANOVA and Bonferroni's correction for multiple testing. D) Three days after the final CCl_4 injection, mice were euthanized and portions of individual livers preserved in formalin for assessment of neutrophil infiltration by immunohistochemistry. Control (Olive oil injected mice) treated livers did not exhibit positive NIMP-R14 staining (C57BL/6 used as representative for each strain), but NIMP-R14-positive neutrophils were detected in C57BL/6, A17 and 17-C6 mice after CCl_4 exposure (red/brown staining, black arrows). Images were taken at 200× magnification. Quantification of NIMP-R14 as described in the Materials and Methods. CV = central vein. N = 2 (olive oil) or 3 (CCl_4) for each strain. Superscripts without a common letter differ from each other, $P<0.05$ as determined with ANOVA and Bonferroni's correction for multiple testing

Table 1

Lieber DeCarli Diet study

	C57BL/6J		A/J		CSS-17		17C-1		17C-6	
	PF	**+E**	**PF**	**+E**	**PF**	**+E**	**PF**	**+E**	**PF**	**+E**
Food intake (ml/day)	11.7±0.1[a]	12.5±0.4[b]	11.9±0.3[a]	12.0±0.2[a]	13.1±0.1[b]	12.0±0.1[a]	13.2±0.3[b]	13.1±0.1[b]	13.1±0.0[b]	12.4±0.1[b]
Blood EtoH (mM)	5.1±0.8[a]	46.8±5.6[b]	8.9±1.7[a]	91.9±2.2[c]	3.4±1.0[a]	38.4±5.6[d]	3.1±0.9[a]	47.9±2.4[b]	4.3±0.4[a]	27.6±2.1[d]

Values are the mean ± SEM for n=4–6 female mice per group. The means in a row with superscripts without a common letter differ from each other, $P<0.05$ as determined with ANOVA and Bonferroni's correction for multiple testing. (PF, pair-fed diet, +E, ethanol-containing diet)

Table 2

Summary of candidate genes

Treatment or Diet	Strain				Potential Genes	
	Parental	CSS	Congenics			
	B6	CSS-17	17C-1 (*Obrq13*)	17C-6 (*Obrq15*)	Candidate genes in *Obrq13*	Candidate genes in *Obrq15*
Chronic Lieber DeCarli EtOH Diet	↑Steatosis ↑ALT/AST	↑Steatosis ↑ALT/AST	↑↑↑Steatosis ↑ALT/AST	↑Steatosis ↑ALT/AST	**Noxo1** Slc5a7 Plg Fndc1	**Nlrc4** Ddx11 Cdkl4 Trip 10
Chronic CCL_4	↑Fibrosis	↓Fibrosis	↑↑↑Fibrosis	↓Fibrosis		
HFSC (100days)	Obese ↑Steatosis IR	Lean IS	Lean IS	Lean ↑Steatosis IR		

By analyzing deep sequencing data for A/J compared to B6 chromosome 17, we identified candidate genes on chromosome 17 that may regulate susceptibility to liver injury in ASH. We selected candidate genes in *Obrq 13* and *Obrq 15* that contained non-consensus SNPs in 5' untranslated region (UTR) or within the gene. For ASH, mice were determined to have steatosis if fed Lieber DeCarli ethanol-containing diet and had statistically significant increase of hepatic triglyceride values over pair fed littermates. Mice were considered to have increased fibrosis if α-SMA measurements in CCl_4 treated mice were significantly increased over olive oil treated mice. Detailed results for these experiments can be found in Table 1 for ethanol feeding trial and Figures 4–7 for CCl_4 treatment. The data for the high fat-simple carbohydrate is summarized from our previously published study of congenics derived from CSS-17 (Millward et al., 2009). These mice were characterized as obese if the weight gain was similar to B6 mice. The mice were considered either insulin sensitive (IS) or insulin resistant (IR) as measured by glucose tolerance tests and HOMA-IR as previously published (Millward et al., 2009).

Alcohol Clin Exp Res. Author manuscript; available in PMC 2014 October 01.